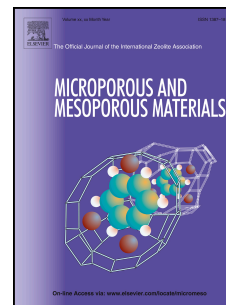


Accepted Manuscript

Extending the range of liquids available for NMR cryoporometry studies of porous materials

Taylor J. Rottreau, Christopher M.A. Parlett, Adam F. Lee, Rob Evans



PII: S1387-1811(18)30410-4

DOI: [10.1016/j.micromeso.2018.07.035](https://doi.org/10.1016/j.micromeso.2018.07.035)

Reference: MICMAT 9045

To appear in: *Microporous and Mesoporous Materials*

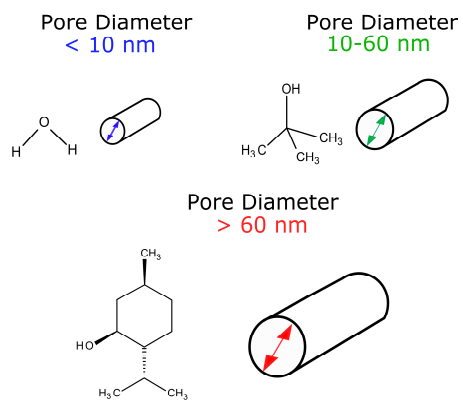
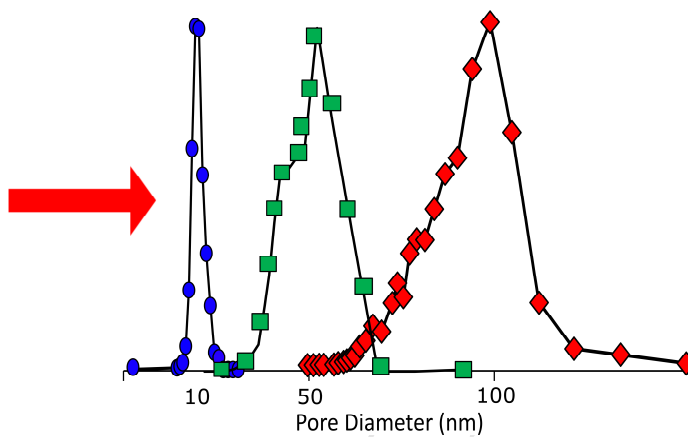
Received Date: 28 April 2018

Revised Date: 13 June 2018

Accepted Date: 24 July 2018

Please cite this article as: T.J. Rottreau, C.M.A. Parlett, A.F. Lee, R. Evans, Extending the range of liquids available for NMR cryoporometry studies of porous materials, *Microporous and Mesoporous Materials* (2018), doi: 10.1016/j.micromeso.2018.07.035.

This is a PDF file of an unedited manuscript that has been accepted for publication. As a service to our customers we are providing this early version of the manuscript. The manuscript will undergo copyediting, typesetting, and review of the resulting proof before it is published in its final form. Please note that during the production process errors may be discovered which could affect the content, and all legal disclaimers that apply to the journal pertain.

SUITABLE CHOICE OF
CRYPOROMETRIC LIQUIDPORE SIZE
DISTRIBUTIONS

ACCEPTED MANUSCRIPT

Extending the Range of Liquids Available for NMR Cryoporometry Studies of Porous Materials

Taylor J. Rottreau[†], Christopher M. A. Parlett[‡], Adam F. Lee[§] and Rob Evans^{†}*

[†]Aston Institute of Materials Research, School of Engineering and Applied Science and

[‡]European Bioenergy Research Institute, Aston University, Birmingham B4 7ET,
United Kingdom.

[§] School of Science, RMIT University, Melbourne VIC3000, Australia.

* Corresponding author. Email address: r.evans2@aston.ac.uk

Abstract

Nuclear magnetic resonance (NMR) cryoporometry, although well established, can be limited by the inability of any one liquid to probe a broad range of pore sizes, a relatively small number of commonly-used probe liquids and the requirement to match the probe liquid to the chemistry of the material being studied. Here we demonstrate, for the first time, the use of menthol and t-butanol as probe liquids in NMR cryoporometry measurements. Using appropriate estimates for the values of the melting point depression constant, k_c , and the non-freezing surface layer, $2s_l$, NMR melting data was converted into pore size distributions. The melting point depression constant for t-butanol is similar to that of cyclohexane; however due to its functionality, t-butanol may be the preferred liquid used to study the porosity of hydrophilic materials. Menthol, having a larger value of k_c , can accurately analyze larger pore sizes up to 100 nm. This represents the first use of menthol and t-butanol to accurately probe pore dimensions in NMR cryoporometry.

Keywords

NMR Cryoporometry
Porous Materials
NMR Characterization
t-butanol
Menthol
Probe liquids

1. Introduction

Nuclear magnetic resonance (NMR) cryoporometry is a well-established technique used to accurately measure the pore size distribution of mesoporous materials [1-6]. Cryoporometry can non-invasively measure the phase transition of a liquid, confined in various pore geometries, in discrete steps [3]. However, a major disadvantage of the technique is that a single liquid cannot probe a wide range of pore sizes or surface chemistry; a range of liquids, with differing thermodynamic properties, are therefore required to span the full range of pores sizes amenable for NMR investigations.

NMR cryoporometry uses the observed depression in melting point of a confined liquid to obtain a pore size distribution, as introduced by Gibbs and Thomson [7-12]. The melting point depression ΔT_m is predicted by Equation 1

$$\Delta T_m = T_m - T_m(x) = \frac{4\gamma_{sl}T_m}{x\Delta H_f\rho_s} \quad (1)$$

$$\Delta T_m = \frac{k_c}{x-2sl} \quad (2)$$

where T_m is the bulk solid melting point, $T_m(x)$ is the melting point of a crystal with diameter x , ΔH_f is the bulk enthalpy of fusion, ρ_s is the density of the solid, and γ_{sl} is the surface energy at the crystal-liquid interface [2]. The parameters in Equation 1 can be collectively reduced to one value, known as the melting point depression constant k_c . Equation 2 takes into account the additional contribution from a non-freezing surface layer, typically labelled as $2sl$.

Values for the two key parameters in cryoporometry analysis, k_c and $2sl$, are seldom agreed upon in the literature. The collection of parameters which define k_c determine the range of pore sizes that a liquid can accurately analyze. An approximation for k_c is obtained from Equation 3:

$$k_c = 2\nu\gamma_{sl} \frac{T_m}{\Delta H_f} \quad (3)$$

where ν is the molar volume of the liquid, γ_{sl} is the surface energy at the crystal-liquid interface, ΔH_f is the bulk enthalpy of fusion, and T_m is the bulk melting point. An estimate for k_c can therefore be obtained if values are known for the molar volume of the liquid, the free energy at the crystal/liquid interface, and the latent heat of melting.

Potential cryoporometric liquids, with estimates for k_c , have been collated by Petrov and Furo [4], including water, cyclohexane, octamethylcyclotetrasiloxane (OMCTS), menthol, and t-butanol. Cyclohexane and water are two of the most common liquids for cryoporometry analysis due to their favourable melting points and suitable melting point depression constants [2, 5, 6, 13-15]. Water ($k_c = 49.5$ K.nm) is well suited for the analysis hydrophilic materials, such as silica, with pore diameters <10 nm, whereas cyclohexane ($k_c = 103.7$ K.nm) is more suited to hydrophobic materials, such as porous glasses, with pore diameters between 10-50 nm. Glasses smaller in size can be pre-treated with hexamethyldisilazane to make the glass more hydrophobic and promote the wetting of cyclohexane [13]. Larger pore diameters can be probed by two methods. The first is to use appropriately smaller temperature steps for liquids which have a relatively high k_c , although this method will still ultimately fall short when the pore diameter exceeds a certain limit. The second is to use a liquid with a much larger

k_c value. OMCTS has been demonstrated as a suitable liquid for larger pore analysis [16]. Despite a similar k_c to cyclohexane, OMCTS can accurately measure the pore size distributions of glass into the micron range when sufficiently small temperature steps are used.

Neither menthol nor t-butanol have been previously used as probe liquids for NMR cryoporometry. The only previous studies of their melting behaviour are provided by Christenson [17], and Qiao and Christenson [18], for t-butanol and menthol respectively. Both studies describe the capillary condensation of the alcohols between mica surfaces and provide estimates of the solid-liquid interfacial tension. With accessible melting points, both liquids are ideal candidates as probe liquids in NMR cryoporometry experiments. In cryoporometry experiments, k_c is typically calibrated against experimental data, however such calibrations are highly susceptible to the choice of fitting function, particularly in estimating the non-freezing surface layer ($2sl$) which can lead to significant errors. We have previously investigated the melting point depression constant, and influence of a non-freezing surface layer, for water confined in mesoporous silica, and applied this methodology to cyclohexane confined within CPGs [6]. Here we extend this methodology to estimate these two parameters for t-butanol and menthol and, hence, demonstrate the suitability of both alcohols for NMR cryoporometry.

2. Experimental

2.1. Materials

Controlled pore glasses were provided by both Sigma-Aldrich (24, 50 and 54 nm) and Prime Synthesis (38, 43, 63 and 100 nm). Their properties are listed in **Table 1**.

2.2. NMR Hardware and Temperature Control

All NMR measurements were carried out on a Bruker Avance spectrometer, equipped with a 5 mm PABBO BB-1H Z-GRD probe, with a frequency of 300 MHz. To obtain low temperatures, a Bruker BVT3200 temperature control system, with a precision of 0.1 K, was used. The cooling system passes a combination of N₂ gas and air over the sample at a flow rate of 400 l/h operating at 4% cooling with the probe heater set to a maximum of 17% output. Before starting experimental work, the temperature control system was calibrated using a deuterated methanol NMR thermometer, producing a calibration relationship between the nominal spectrometer temperature and actual sample temperature [19]. Further calibrations were performed to determine the stability of the temperature at a given nominal spectrometer temperature and also the time taken for a given temperature change to occur. Before the start of a cryoporometry experiment, the cooling system was allowed to equilibrate with the probe heater. The temperature control unit was optimized to ensure that over- and undershoot of the sample temperature was minimized effectively. Furthermore, the probe was tuned and matched in areas out of sample phase transition to account for the significant temperature changes.

The NMR signal intensities between pore and bulk melting regions have been corrected to account for the effect of Curie's law, where the signal intensity decreases with increasing temperature outside of phase transformations [20]. The intensities are then further normalized to a value where all of the confined water is liquid and the bulk water remains frozen.

2.3. NMR Cryoporometry

Cryoporometry measurements were made using the Carr-Purcell-Meiboom-Gill (CPMG) pulse sequence [21, 22], comprising a basic spin echo, and carefully selected delay time, Δ , to differentiate between the solid and liquid phases of the sample (pulse sequence can be found in supporting information, **Figure S1**). Total delay times of 4 ms and 40 ms for menthol and t-butanol respectively successfully isolated the liquid signal. The sample temperature was reduced until the entire sample was frozen, evidenced by the loss of all liquid signal. The temperature was then increased in increments of 0.2 – 0.5 K, to initiate and observe the phase transition from solid to liquid, using a minimum equilibration time of 10 min at each temperature to stabilize the signal intensity. Each acquisition comprised of 8 transients of 8192 complex data points.

The melting point depressions obtained by NMR cryoporometry can be converted into pore size distributions using the methodology detailed by Strange et al [1], using Equation 4:

$$\frac{dv}{dx} = \frac{k_c}{x^2} \cdot \frac{dv}{dT} \quad (4)$$

where the change in liquid volume with temperature is denoted by dv/dT , k_c is the melting point depression constant, and x is the pore diameter.

2.4. NMR Relaxometry

Transverse relaxation time, T_2 , distributions for the liquids were obtained using the PROJECT pulse sequence (pulse sequence, and typical timing parameters, can be found in supporting information, **Figure S2**) [23]. Each acquisition comprised of 8 transients of 16384 complex data points, with a maximum experimental time of 8 minutes. The total delay time was varied from over 10 increments, with exact timings dependent on the liquid used and the phase of the sample. Relaxation time distributions were calculated using CONTIN. [24]

3. Results & Discussion

To be considered a viable probe liquid for cryoporometry experiments, the phase transition from solid to liquid has to be relatively simple, with the absence of any intermediate stages or plastic crystals, crystalline structures with high molecular mobility [1]. There must also be measurable differences in transverse relaxation time between the pore liquid and the bulk liquid. In order to assess the melting behaviour of *t*-butanol and menthol, hysteresis data was acquired for the bulk liquids (supporting information, **Figure S3**). For both alcohols, as well as the cyclohexane standard, the transition from solid to liquid occurred over a narrow range of temperatures and was free of any secondary phases. The freezing of the liquids, although at different temperatures due to the well-established super-cooling phenomena of liquids in pores [3], also occurred over a narrow range of temperatures.

The confining environment of a pore may contribute to the complexity of the melting process. In any event, there needs to be a difference between the transverse

relaxation times of the solid and liquid phases such that they can be differentiated by the use of a spin-echo NMR experiment. In order to evaluate this, T_2 distributions were acquired for all three liquids over a range of temperatures near that particular liquid's melting point. **Figure 1** illustrates the increase in T_2 times going from a solid through to a pore-constrained liquid. In all three cases, the transition is clear and there is a distinct difference between the solid (ca. 0.001 s) and liquid (ca. 0.01-0.1 s) T_2 times. Hardware restrictions meant that the T_2 times of the solids far below the pore melting region could not be measured, due to problems in acquiring the required spectral widths. In spite of this, **Figure 1** still highlights the relatively simple transitions between solid and liquid for both alcohols and the greater than ten-fold differences in T_2 . Measurements over a wider range of temperatures than shown in **Figure 1** were acquired and T_2 distributions for these additional temperatures are provided in the supporting information (**Figures S4-6**).

While the 100 fold difference in T_2 times observed for cyclohexane is ideal, the differences between the T_2 times of the solid and liquid phases of alcohols used in this work allow for the two states of matter to be distinguished by a spin-echo experiment. Appropriate timings for the spin-echo NMR experiments are still crucial for accurately determining the phase transition temperature of a liquid melting in a confined environment. The total experimental delay time in a spin-echo experiment, Δ , allows the solid and liquid signals to be separated due to the significant differences between the T_2 times of the two phases, as illustrated in **Figure 2**.

If the optimal delay time is not used, then the acquired melting curves will not reflect the true pore size distributions of the materials. A simple procedure to identify the optimal delay time is to first reduce the temperature of the sample so that both bulk and

confined liquid freeze. The temperature is then increased incrementally to ensure that only the confined material melts, and a freezing curve is acquired at a series of different delay times. Using a delay time which is too long will result in the loss of the liquid signal from smaller pores, and the resulting melting curve will not reflect a sigmoidal function. This is illustrated for menthol confined in 50 nm mean diameter porous glass in **Figure 2**, where the use of long delay times (40 ms) would skew the pore size distribution towards larger pores. Too short a delay time would result in an apparent phase transition at a lower temperature than expected, illustrated for t-butanol confined in 50 nm mean diameter porous glass, also in **Figure 2**, where signal intensity is observed <285 K when a 4 ms delay is used.

In order to successfully convert good quality NMR melting curve data into a pore size distribution, both the melting point depression constant, k_c , and the thickness of the non-freezing surface layer, $2sl$, need to be known. Using the method introduced in reference 6, **Figure 3** plots the inverse melting point depressions obtained in this work, and from two literature references [17, 18], against the pore diameter obtained by other methods. A one-parameter fit for $2sl$ for menthol and t-butanol using Equation 2 (using data collected in **Table 2** to predict values for k_c from Equation 3), gives estimates for this layer of 1.9 ± 1.1 and 1.7 ± 1.0 nm respectively. Both fits have R^2 values of 0.99. Note that the additional source of data is not an NMR cryoporometry study. This work demonstrates the use and analysis of literature melting point depression data and the additional insight from and application of these sources of data.

The NMR melting curves for both t-butanol and menthol confined within CPG63 were acquired and both follow the expected sigmoidal shape for such data. The melting curves, with cyclohexane as a comparison, are depicted in **Figure 4(a)**, together with

their corresponding pore size distributions, produced using Equation 4, in **Figure 4(b)**. The pore size measurements are all in good agreement. An average pore diameter of 61.5 nm was obtained using cyclohexane, 62.0 nm using t-butanol, and 64.8 nm using menthol. Of the three liquids, cyclohexane has a phase transition that occurs over the narrowest temperature range, whereas both alcohols have relatively broader melting points, reflected in their wider pore size distributions. Despite having a phase transition that occurs over a wider temperature range, the size distribution from menthol in CPG63 is narrower than that obtained from t-butanol. This may reflect that the latter probe molecule is approaching the upper limit of the pore sizes it can measure; each temperature step leads to a larger gap between the corresponding pore diameters as the temperature approaches T_m , an effect that dominates the pore size distribution of CPG63 as measured by t-butanol.

Pore size distributions were acquired using both menthol and t-butanol for the remaining controlled pore glasses described in **Table 1**. **Figure 5** compares the pore sizes measured using NMR cryoporometry, for the materials that both liquids were able to accurately measure, with those supplied by the manufacturer. Both alcohols were used to obtain pore size measurements in good agreement with manufacturers' reported values. The pore size distributions obtained for every CPG sample measured by both liquids can be found in **Figures S7**. As the pore sizes increase, broader temperature ranges for each melting curve are acquired resulting in broader pore size distributions, especially for t-butanol in CPG63. This behaviour is similar to that observed using OMCTS as a probe liquid [16]. Menthol also appears to slightly underestimate pore diameters <50 nm, for which t-butanol may be better suited to analysing.

However, neither cyclohexane nor t-butanol were able to accurately measure the size distribution of the largest pore CPG100 material, reflecting their similar melting point depression constants (*ca.* 100 K.nm) and subsequent limited ability to probe larger pore sizes. Menthol, which has the largest k_c value of the liquids used in this study, was used to successfully measure the pore sizes of the widest bore controlled pore glass in this study, CPG100, as shown in **Figure 6**. The k_c value estimated for menthol renders it a potential probe liquid for analysing even larger pores than those reported in this work. However, disadvantages of menthol do include longer waiting times to achieve equilibrium during the melting process, perhaps necessitating fewer temperature steps to maintain a practical total experimental time, or experimental set-ups capable of automated, accurate 0.1 K temperature increments.

Conclusions

Although NMR cryoporometry has been established as an accurate pore size determination technique, it has its limitations. These include the inability of any one liquid to analyse a wide pore size range, a relatively small number of tried and tested probe liquids and a requirement to match the probe liquid to the chemistry of the solid being studied. In this work, we have demonstrated for the first time, the ability of menthol and t-butanol to be introduced as probe liquids for cryoporometry analysis.

The melting point depression constants, k_c , obtained for both alcohols were estimated according to their thermodynamic parameters, enabling a value for the non-freezing surface layer, $2sl$, to be predicted based on recently established methodology. The estimated melting point depression constant for t-butanol is similar to that of the established probe liquid, cyclohexane. Its advantage is in being able to penetrate into materials more easily where the hydrophobicity of cyclohexane may prevent it from

doing so. Menthol has a significantly larger k_c than most liquids currently reported in NMR cryoporometry analysis. It appears to slightly underestimate smaller pore sizes; however, with the correct experimental set-up, it is possible to probe larger pore sizes effectively.

This work is the first demonstration of the use of t-butanol and menthol in NMR cryoporometry experiments, and demonstrates that pore sizes up to 100 nm, and potentially beyond, can be measured using the latter alcohol. There is potential for wide application of this methodology in more complex samples of engineering and scientific interest, such as templated silica [25], templated apatite [26] and hyper-crosslinked polymers [27]. The use of different probe liquids, with different functional groups and chemistry, renders NMR cryoporometry a versatile complement to N₂ porosimetry.

Acknowledgments

Financial support for a Ph.D. studentship from the School of Engineering and Applied Science, Aston University, is gratefully acknowledged. R.E and T.J.R would like to thank LGC Prime Synthesis for supplying CPG samples and Amin Osatiashtiani for help with the revision of the manuscript. A.F.L. and C.M.A.P. were supported by the Engineering and Physical Sciences Research Council (Grant Number EP/N009924/1).

To access the research data supporting this publication, please see:

<http://doi.org/10.17036/researchdata.aston.ac.uk.00000331>.

References

- (1) J.H. Strange, M. Rahman, E.G. Smith, *Phys. Rev. Lett.* 71 (1993) 3589-3591.
- (2) C.L. Jackson, G.B. McKenna, *J. Chem. Phys.* 93 (1990) 9002-9011.
- (3) J. Mitchell, J.B.W. Webber, J.H. Strange, *Phys. Rep.* 461 (2008) 1-36.

- (4) O.V. Petrov, I. Furo, *Prog. Nucl. Mag. Res. Sp.* 54 (2009) 97-122.
- (5) E.W. Hansen, R. Schmidt, M. Stöcker, *J. Phys. Chem.* 100 (1996) 11396-11401.
- (6) T.J. Rottreau, C.M.A. Parlett, A.F. Lee, R. Evans, *Micropor. Mesopor. Mat.* 264 (2018) 265-271.
- (7) J.W. Gibbs, *The Collected Works of J. Willard Gibbs*. Longmans, Green & Co, London, 1928.
- (8) J.W. Gibbs, *The Scientific Papers of J. Willard Gibbs, New Dover Edition. Thermodynamics. Vol. 1*, Longmans, Green & Co, 1906.
- (9) J. Thomson, *Trans. Roy. Soc.* 5 (1849) 575-580.
- (10) J. Thomson, *Proc. Roy. Soc.* 11 (1862) 473-481.
- (11) J.J. Thomson, *Applications of Dynamics to Physics and Chemistry*. Macmillan & Co, London, 1888.
- (12) W. Thomson, *Phil. Mag. Series.* 42 (1871) 452-488.
- (13) D.W. Aksnes, L. Kimtys, *Appl. Magn. Reson.* 23 (2002) 51-62.
- (14) D.W. Aksnes, K. Førlund, L. Kimtys, *J. Mol. Struct.* 708 (2004) 23-31.
- (15) O.V. Petrov, I. Furo, *Micropor. Mesopor. Mat.* 136 (2010) 83-91.
- (16) D. Vargas-Florencia, O.V. Petrov, I. Furo, *J. Colloid. Interf. Sci.* 305 (2007) 280-285.
- (17) H. Christenson, K., *J. Phys. Condens. Matter.* 13 (2001) 95-133.
- (18) Y. Qiao, H.K. Christenson, *Phys. Rev. Lett.* 86 (2001) 3807-3810.
- (19) M. Findeisen, T. Brand, S. Berger, *Magn. Reson. Chem.* 45 (2007) 175-178.
- (20) A. Abragam, *The Principles of Nuclear Magnetism*. Clarendon Press, Oxford, 1961.
- (21) H.Y. Carr, E.M. Purcell, *Phys. Rev.* 94 (1954) 630-638.
- (22) S. Meiboom, D. Gill, *Rev. Sci. Instrum.* 29 (1958) 688.
- (23) J.A. Aguilar, M. Nilsson, G. Bodenhausen, G.A. Morris, *Chem. Comm.* 48 (2012) 811-3.
- (24) S.W. Provencher, *Comput. Phys. Commun.* 27 (1982) 229-242.
- (25) J.P. Dacquin, A.F. Lee, C. Pirez, K. Wilson, *Chemical Communications.* 48 (2012) 212-214.
- (26) Y.S. Pek, S. Gao, M.S.M. Arshad, K.-J. Leck, J.Y. Ying, *Biomaterials.* 29 (2008) 4300-4305.
- (27) L. Tan, B. Tan, *Chemical Society Reviews.* 46 (2017) 3322-3356.
- (28) R.H. Stokes, R.P. Tomlins, *J. Chem. Thermodyn.* 6 (1974) 379.
- (29) E.S. Domalski, E.D. Hearing, *J. Phys. Chem. Ref. Data.* . 25 (1997) 1501.
- (30) J.S. Chickos, C.M. Braton, D.G. Hesse, *J. Org. Chem.* 56 (1991) 927-938.

Tables

Table 1. Characterisation of controlled pore glasses: Pore diameter, pore volume, grain size, and specific surface area (from N₂ porosimetry). Data supplied by Sigma-Aldrich and Prime Synthesis.

Glass	Pore diameter (nm)	Pore volume (cm ³ .g ⁻¹)	Grain size (mesh)	Specific surface area (m ² .g ⁻¹)
CPG24	24.0	-	20-80	-
CPG38	38.2	1.10	120-200	113
CPG43	42.8	1.40	120-200	130
CPG50	50.0	0.96	120-200	51
CPG54	54.0	1.06	120-200	44
CPG63	62.6	1.20	120-200	79
CPG100	99.6	1.40	120-200	55

Table 2. Selected thermodynamic properties of selected cryoporometric liquids.

Liquid	v (m ³ .mol ⁻¹)	T_m (K)	γ_{sl} (N.m ⁻¹)	ΔH_f (kJ.mol ⁻¹)	k_c (K.nm)
Cyclohexane	108.7	278-280	0.030 [2]	2.7 [28]	103.7
t-Butanol	95.6	296-299	0.014 [17]	6.7 [29]	119.2
Menthol	175.6	305-309	0.024 [18]	11.9 [30]	219.3

Figures

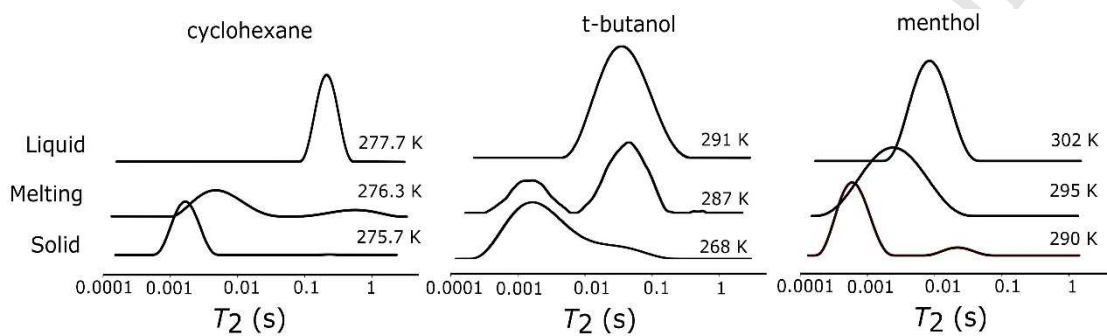
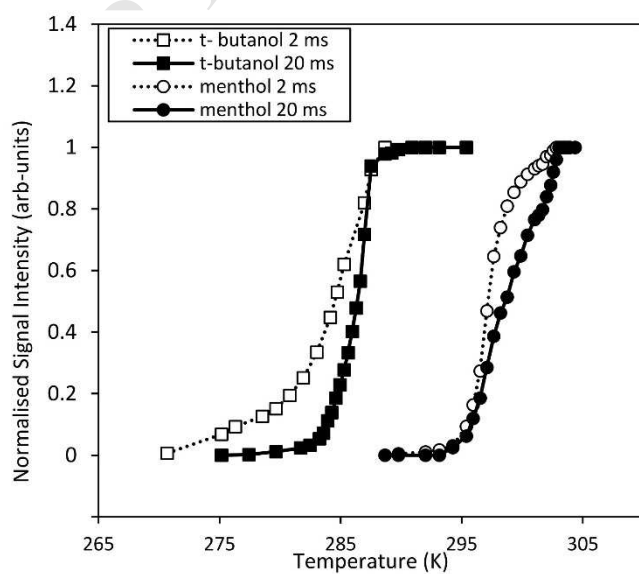
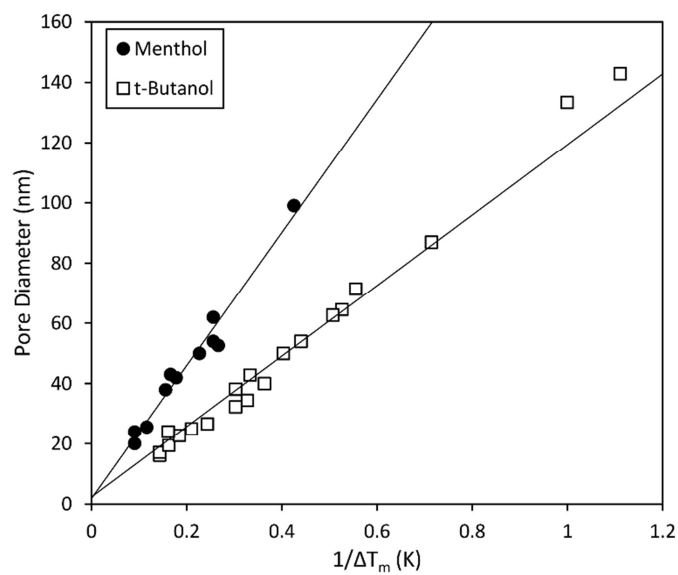
Figure 1.**Figure 2.**

Figure 3.**Figure 4.**

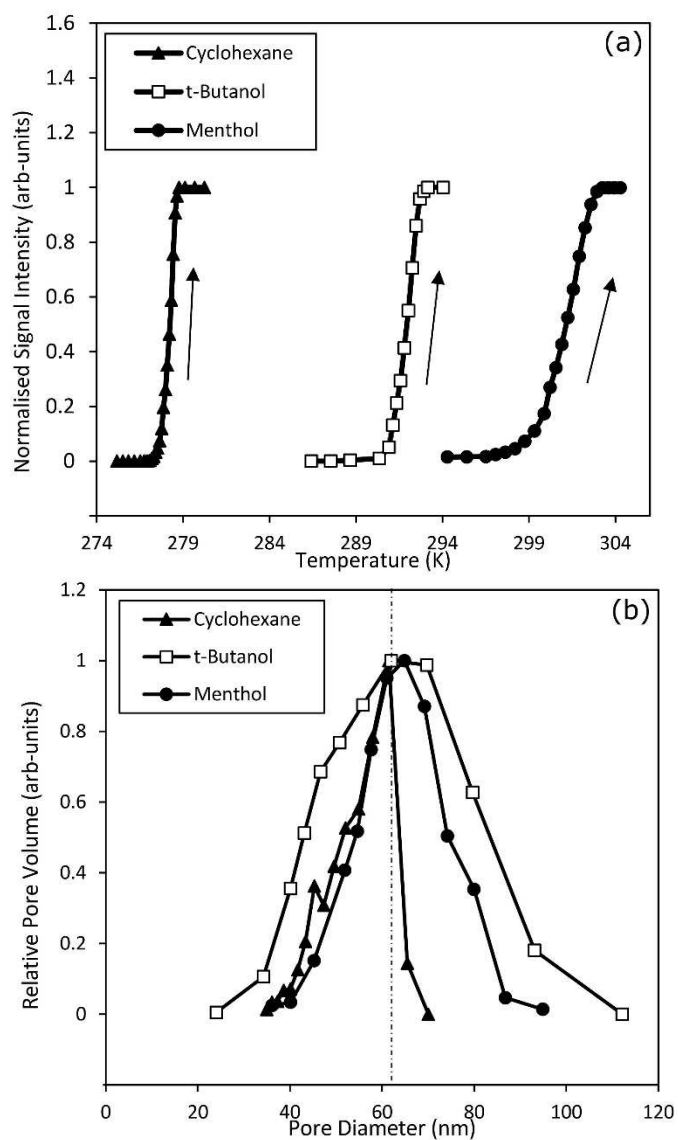


Figure 5.

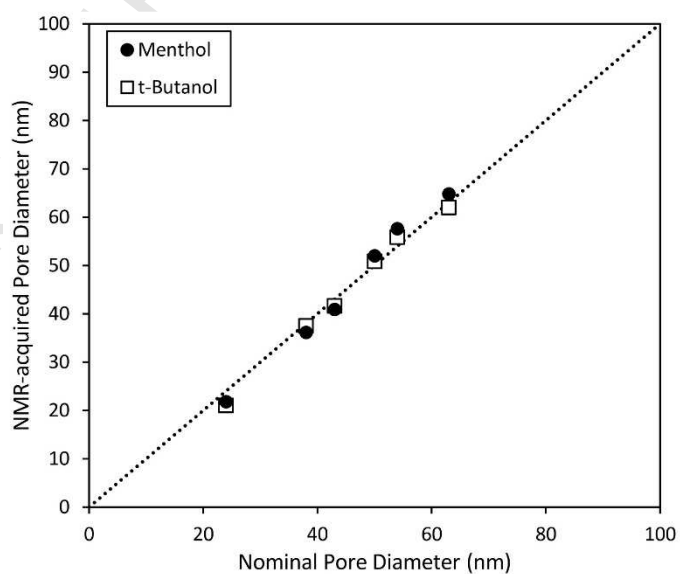


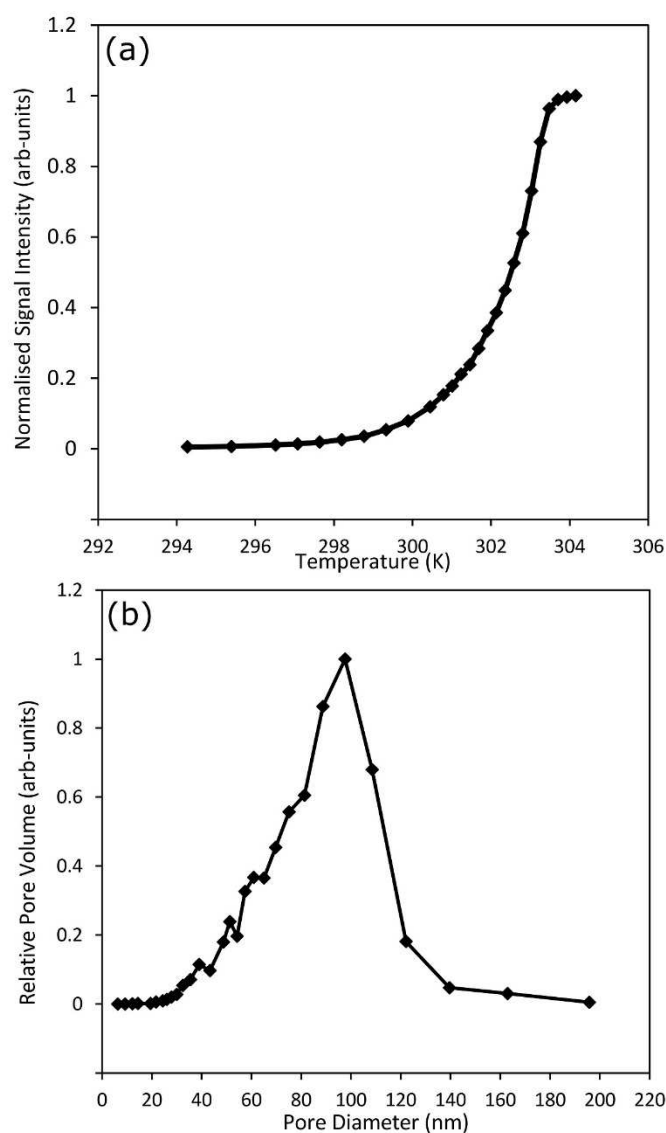
Figure 6.

Figure Captions

Figure 1. Indicative T_2 distributions for cyclohexane, t-butanol and methanol, confined within the pores of CPG24, when solid, during the pore melting transition and when all of the species inside of the pore has melted.

Figure 2. Melting curves for t-butanol (squares) and menthol (circles) acquired using two different spin-echo delays: 40 ms (filled) and 4 ms (hollow).

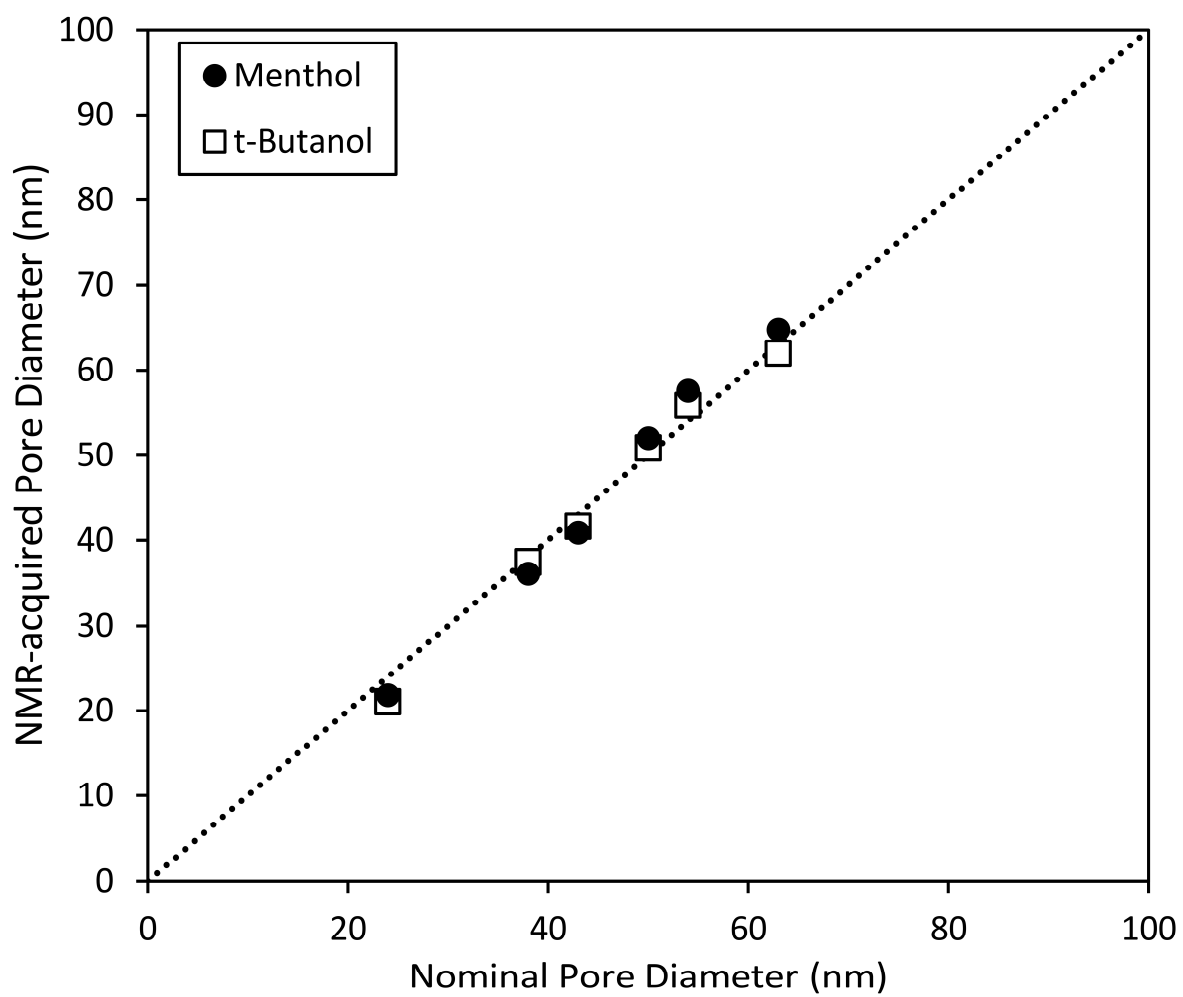
Figure 3. Plot of average pore diameter versus the inverse of the measured melting point depression for cryoporometry data obtained in the present work and references 14

and 16. Using the method of reference 6, the intercept of the linear fits yield values of 1.9 nm and 1.7 nm for the thickness of the non-freezing surface layer for menthol and t-butanol respectively.

Figure 4. (a) Melting curves for cyclohexane, t-butanol, and menthol in CPG63 and (b) corresponding pore size distributions for the three liquids, obtained using Equation 4.

Figure 5. Comparison of pore sizes, measured using NMR cryoporometry, with nominal pore sizes as supplied by the manufacturer for a set of 5 controlled pore glass samples (described in **Table 1**).

Figure 6. (a) The NMR melting curve for menthol confined in CPG100 and (b) the subsequent pore size distribution using a k_c value of 219.3 K.nm and a $2sl$ of 1.9 nm.



ACCEPTED

Highlights

- Potential liquids for NMR cryoporometry expanded to include menthol and t-butanol.
- Reliable estimates of parameters, k_c and $2s_l$, obtained for both liquids.
- Demonstration of use for both liquids over range of pore sizes from 20 to 100 nm.

ACCEPTED MANUSCRIPT